Society For Biomaterials

Effect of cell-seeded hydroxyapatite scaffolds on rabbit radius bone regeneration

C. R. Rathbone,[1] T. Guda,[1,2] B. M. Singleton,[2] D. S. Oh,[2,3] M. R. Appleford,[2] J. L. Ong,[2] J. C. Wenke[1]

[1]Extremity Trauma and Regenerative Medicine, U.S. Army Institute of Surgical Research, Ft. Sam Houston, Texas
[2]Department of Biomedical Engineering, The University of Texas at San Antonio, San Antonio, Texas
[3]Department of Orthopaedic Surgery, Columbia University Medical Center, New York, New York

Received 8 March 2013; revised 31 May 2013; accepted 5 June 2013
Published online 22 June 2013 in Wiley Online Library (wileyonlinelibrary.com). DOI: 10.1002/jbm.a.34834

Abstract: Highly porous hydroxyapatite (HA) scaffolds were developed as bone graft substitutes using a template coating process, characterized, and seeded with bone marrow-derived mesenchymal stem cells (BMSCs). To test the hypothesis that cell-seeded HA scaffolds improve bone regeneration, HA scaffolds without cell seeding (HA-empty), HA scaffolds with 1.5×10^4 BMSCs (HA-low), and HA scaffolds with 1.5×10^6 BMSCs (HA-high) were implanted in a 10-mm rabbit radius segmental defect model for 4 and 8 weeks. Three different fluorochromes were administered at 2, 4, and 6 weeks after implantation to identify differences in temporal bone growth patterns. It was observed from fluorescence histomorphometry analyses that an increased rate of bone infiltration occurred from 0 to 2 weeks ($p < 0.05$) of implantation for the HA-high group (2.9 ± 0.5 mm) as compared with HA-empty (1.8 ± 0.8 mm) and HA-low (1.3 ± 0.2 mm) groups. No significant differences in bone formation within the scaffold or callus formation was observed between all groups after 4 weeks, with a significant increase in bone regenerated for all groups from 4 to 8 weeks (28.4% across groups). Although there was no difference in bone formation within scaffolds, callus formation was significantly higher in HA-empty scaffolds (100.9 ± 14.1 mm^3) when compared with HA-low (57.8 ± 7.3 mm^3; $p \leq 0.003$) and HA-high (69.2 ± 10.4 mm^3; $p \leq 0.02$) after 8 weeks. These data highlight the need for a better understanding of the parameters critical to the success of cell-seeded HA scaffolds for bone regeneration. © 2013 Wiley Periodicals, Inc. J Biomed Mater Res Part A: 102A: 1458–1466, 2014.

Key Words: hydroxyapatite, rabbit radius, mesenchymal stem cells, bone, callus

How to cite this article: Rathbone CR, Guda T, Singleton BM, Oh DS, Appleford MR, Ong JL, Wenke JC. 2014. Effect of cell-seeded hydroxyapatite scaffolds on rabbit radius bone regeneration. J Biomed Mater Res Part A 2014:102A:1458–1466.

INTRODUCTION

Long bone fractures and their potential complications, including bony nonunions, remain a significant financial, emotional, and physical burden despite years of research to address this problem. The search for substitutes for autologous bone grafting applications has led to the development of scaffolds composed of a variety of materials, including hydroxyapatite (HA), a well-known biocompatible calcium phosphate ceramic. HA has several qualities that may make it an alternative option for the treatment of long-bone fractures, including its ability to integrate with host bone and the possession of elastic properties that is similar to native bone.[1] The archetypical approach for achieving maximal bone tissue regeneration has been to integrate combinations of osteoconductive scaffolds, an osteoinductive milieu, and an osteogenic cell population to maximize fracture healing.[2] With regard to HA scaffolds, one of its putative roles in bone regeneration is to act as an osteoconductive structure. Some investigators have shown that the bone restorative potential of HA scaffolds can further be improved when combined with mesenchymal stem cells (MSCs).[3–5] The finding that repair of long-bone defects is accelerated in patients if implanted with osteoprogenitor cell-seeded HA scaffolds gives clinical support for the cell-based approaches utilizing HA scaffolds.[6] Although tissue-engineering strategies, including cell seeding, have predominantly led to improved bone regeneration, cell-seeded scaffolds have also been suggested to performed no better than, or are inferior to, empty scaffolds.[7,8] The lack of performance by cell-seeded HA scaffolds in some studies raises the possibility that the use of cell-seeded HA scaffolds may result in a spectrum of possible *in vivo* outcomes, especially when considering the wide range of animal models used. The utility of MSCs for bone tissue engineering has extended beyond its differentiation potential, including their modulatory effects on the host tissue through the secretion of trophic factors.[9] For example, it was recently reported that the seeding of HA scaffolds with MSCs influenced the type of ossification (endochondral versus intramembranous) and the cascade of bone formation, which may be due, at least

Correspondence to: C. R. Rathbone; e–mail:christopher.r.rathbone.civ@mail.mil

Report Documentation Page

Form Approved
OMB No. 0704-0188

1. REPORT DATE	2. REPORT TYPE	3. DATES COVERED
01 MAY 2014	**N/A**	**-**

4. TITLE AND SUBTITLE	5a. CONTRACT NUMBER
Effect of cell-seeded hydroxyapatite scaffolds on rabbit radius bone regeneration	5b. GRANT NUMBER
	5c. PROGRAM ELEMENT NUMBER
6. AUTHOR(S)	5d. PROJECT NUMBER
Rathbone C. R., Guda T., Singleton B. M., Oh D. S., Appleford M. R., Ong J. L., Wenke J. C.,	5e. TASK NUMBER
	5f. WORK UNIT NUMBER
7. PERFORMING ORGANIZATION NAME(S) AND ADDRESS(ES)	8. PERFORMING ORGANIZATION REPORT NUMBER
United States Army Institute of Surgical Research, JBSA Fort Sam Houston, Tx 78234	
9. SPONSORING/MONITORING AGENCY NAME(S) AND ADDRESS(ES)	10. SPONSOR/MONITOR'S ACRONYM(S)
	11. SPONSOR/MONITOR'S REPORT NUMBER(S)

12. DISTRIBUTION/AVAILABILITY STATEMENT
Approved for public release, distribution unlimited

13. SUPPLEMENTARY NOTES

14. ABSTRACT

15. SUBJECT TERMS

16. SECURITY CLASSIFICATION OF:			17. LIMITATION OF ABSTRACT	18. NUMBER OF PAGES	19a. NAME OF RESPONSIBLE PERSON
a. REPORT	b. ABSTRACT	c. THIS PAGE			
unclassified	**unclassified**	**unclassified**	**UU**	**10**	

in part, to the progenitor cells that they recruit.[10,11] Importantly, these effects are dependent on the differentiation status of the implanted cells and can be affected by the conditions under which cell cultures are expanded.[10,11] As a result, these differences may potentially be attributed to changes in the secretion profile of trophic factors.[10,12]

Other plausible explanations for the variable effects of cell-seeded scaffolds on bone formation include different seeding densities, thereby possibly resulting in variations of secreted MSC trophic factors.[4,13,14] In support of this contention, temporal differences in gene expression were observed when MSCs were seeded at low, medium, and high densities, suggesting the need and the importance of understanding seeding density in a three-dimensional (3D) scaffold.[15] As such, in order for the beneficial effects of scaffold seeding to be fully realized, a detailed understanding of the conditions required for maximal bone regeneration needs to be evaluated.[16] In the current study, porous interconnected HA scaffolds were seeded with bone marrow-derived MSCs (BMSCs), and the construct was implanted in a rabbit radius segmental defect model to test the hypothesis that cell-seeded HA scaffolds improve bone regeneration. Using two different cell seeding densities, a secondary objective was to determine the effect of seeding density on bone regeneration.

MATERIALS AND METHODS

Animals

This study was conducted in compliance with the Animal Welfare Act and the Implementing Animal Welfare Regulations and in accordance with the principles of the Guide for the Care and Use of Laboratory Animals. All animal procedures were approved by the U.S. Army Institute of Surgical Research Animal Care and Use Committee. Female skeletally matured New Zealand white rabbits were housed in a vivarium accredited by the Association for Assessment and Accreditation of Laboratory Animal Care International.

Experimental design

To determine whether seeding HA scaffolds with BMSCs improves bone regeneration and whether the extent of bone regeneration was affected by seeding density, rabbits with a 1-cm radial defect were implanted with one of the following three scaffolds: (1) HA scaffold alone (HA-empty), (2) HA scaffold seeded with a relatively low density of cells (1.5×10^4 ; HA-low), and (3) HA scaffold seeded with a relatively high density of cells (1.5×10^6; HA-high). With a sample size of 10 scaffolds per group, the animals were euthanized at 4 and 8 weeks after surgery. Fluorochrome injections were performed at 2, 4, and 6 weeks after injection to evaluate the rate of bone formation within the scaffold. Histological analyses and microcomputed tomography (μCT) were performed on these scaffolds 4 and 8 weeks after implantation.

Scaffold preparation

Using a previously described template coating process, porous fully interconnected HAp scaffolds were prepared.[17,18] Briefly, polyurethane sponges (EN Murray, Denver, CO) with a mean pore size of 340 μm were used as templates for the scaffolds. The templates were designed to mimic a 10-mm rabbit radius segmental defect model and had an elliptical cross section to match explanted bone, which averaged a 5-mm major axis and a 3-mm minor axis. The templates were then coated twice in distilled water-based HA slurry. Coated sponges were then vacuum dried overnight before sintering to 1230°C for 3 h in a high-temperature furnace (Thermolyne, Dubuque, IA). All scaffolds were sterilized with ethylene oxide gas before implantation. Before animal implantation, the porosity of the scaffolds was characterized by using helium pycnometry (Accupyc 1340; Norcross, GA) and μCT analysis on a Skyscan 1076 (Skyscan, Kontich, Belgium).[19]

BMSC isolation and culture

To harvest bone marrow aspirates from rabbits, the area overlying the tibia and iliac crest was aseptically prepared, and a 15-gauge aspiration needle was inserted into the bone marrow compartment using an EZ-IO drill (Vidacare Corporation, Shavano Park, TX) into two female New Zealand white rabbits. Bone marrow aspirates were collected with a syringe containing heparin (1000 units) (Sigma) and the volume of aspirate limited to decrease peripheral blood dilution.[20] After the addition of Ficoll-Paque PLUS (Stem Cell Technologies), aspirates were centrifuged at 500*g* for 10 min. The buffy coat layer was removed and washed by centrifuging two times for 10 min at 500*g* in phosphate-buffered saline (PBS) containing 2 m*M* of ethylenediaminetetraacetate (EDTA). The nucleated cells were seeded on tissue culture treated flasks in alpha minimum essential medium (alpha-MEM) supplemented with 20% fetal calf serum (FCS), 100 μg/mL streptomycin, 100 U/mL penicillin, and 2 m*M* L-glutamine. After 48 h, nonadherent cells were removed; media were changed twice weekly until 75% confluent, at which time they were frozen (passage 0). Cells were later thawed and expanded in alpha-MEM supplemented with 20% FCS, 100 μg/mL streptomycin, 100 U/mL penicillin, and 2 m*M* L-glutamine. At passage 3 or 4, cells were detached with 0.25% trypsin and 1 m*M* EDTA, counted with a hemacytometer, and used to seed scaffolds.

Cell characterization

A subset of cultures was seeded on to tissue culture plates and treated with the following osteogenic induction media: ascorbic acid (50 μg/mL), β-glycerophosphate (5 m*M*), and dexamethasone (10 n*M*); or with adipogenic induction media: isobutylmethylxanthine (0.5 m*M*) indomethacin (200 μ*M*), insulin (10 μ*M*), dexamethasone (1 μ*M*), and ciglitazone (10 μ*M*) in Dulbecco's MEM containing 10% FCS, 100 μg/mL streptomycin, 100 U/mL penicillin, and 2 m*M* L-glutamine. After 3 weeks of culture, cells were stained with Alizarin Red or Oil Red-O to confirm their osteogenic and adipogenic differentiation potential, respectively.

Scaffold seeding

HA scaffolds were seeded 24 h before surgery with 1.5×10^4 (HA-low) and 1.5×10^6 (HA-high) BMSCs. This density approximates that previously described by Kruyt et al.,[13]

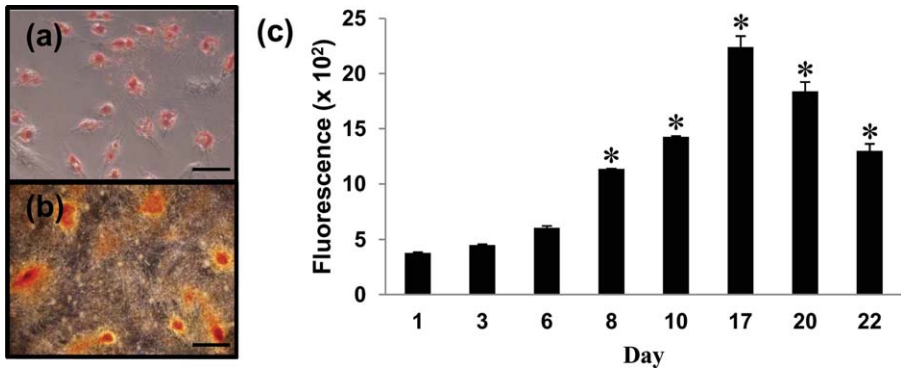

FIGURE 1. Verification of the differentiation potential of the rabbit BMSCs and scaffold seeding procedure. A subset of rabbit MSCs used in the study maintained their multidifferentiation potential as demonstrated by (a) adipogenic and (b) osteogenic differentiation assessed after 3 weeks of culture. (c) Human bone marrow stromal cells seeded on hydroxyapatite scaffolds increased cell number over 22 days. *Significantly different than day 1 ($p < 0.05$). Bar = 100 μM. [Color figure can be viewed in the online issue, which is available at wileyonlinelibrary.com].

where differences in cell density on porous biphasic calcium phosphate resulted in different levels of bone formation in ectopically implanted constructs *in vivo*. All scaffolds (10 × 5 mm) were placed in 48-well plates and treated with vacuum in 0.75-mL 20% FCS, 100 μg/mL streptomycin, 100 U/mL penicillin, and 2 m*M* L-glutamine for 30 min. Cells were seeded perpendicularly in 20 μL of media to one side at four different locations along the scaffold. The scaffold was turned over 10 min later, and the process was repeated. Two hours later, 0.25 mL of the same medium was added to the scaffold. The effectiveness of the scaffold seeding was verified using human bone marrow stromal cells (STEMCELL Technologies, Vancouver, Canada). Briefly, 7.5×10^3 cells were seeded on to 5 × 5 mm scaffolds in 24-well plates and then transferred to a 48-well plate containing the media described above. The scaffolds used for seeding verification were one-half the length of those used for the study *in vivo*; therefore, one-half the number of cells were used to maintain the appropriate seeding density. For seeding verification, cells were cultured for 22 days. The relative number of live cells was measured by using the CellTiter-FluorTM (Promega) cell viability assay similar to the manufacturer's recommendation.

Surgery

A unilateral 10-mm segmental defect was created in the left radial diaphysis similar to that previously described.[18] Briefly, following a 20-mm incision over the middle third of the radius and dissection of the overlying tissues to expose the radial diaphysis, a 10-mm segmental defect was created with an oscillating saw under copious irrigation with normal saline. The defect site was implanted with the scaffold appropriate to the group; immediately after implantation, the soft tissues were approximated with a continuous 2-0 Vicryl (Ethicon, Somerville, NJ), and the skin was closed with deep dermal stitches using a 3-0 Vicryl (Ethicon). Internal fixation was not necessary because of the fibro-osseous syndesmosis between the ulna and the radius. Immediately after surgery and at the time of killing, radiographs were made of the defect limbs. Surgeries that resulted in a sum distance between the proximal and the distal interface between the scaffold and radius > 1.25 mm based on radiographic evaluation of the surgery following implantation were not included. Thus, the following sample sizes were used for all μCT and histological analyses: 4 week HA-empty (n = 9), 4 week HA-low (n = 9), HA-high (n = 9), 8 week HA-empty (n = 6), 8 week HA-low (n = 10), and 8 week HA-high (n = 8).

Polyfluorochrome sequential labeling and histomorphometry

Rabbits received sequential fluorochrome labels at 2 weeks (calcein green, 10 mg/kg intramuscular), 4 weeks (xylenol orange, 60 mg/kg intramuscular), and 6 weeks (teracycline, 25 mg/kg intramuscular) following scaffold implantation to evaluate new bone formation in the scaffolds. The dosages, route, and timing of fluorochrome administration were similar to that previously described.[21,22] At 4 and 8 weeks after scaffold implantation, specimens were removed and placed in formalin. Tissue blocks containing scaffolds were later processed through a dehydration and infiltration method (Exakt, Oklahoma City, OK) for 14 d via a tissue processer (Leica TP1020 system; Bannockburn, IL). Samples were then embedded in photocuring resin (Technovit 7200 VLC;, Kulzer, Germany) and polymerized under blue light for 24 h. Block samples were adhered to a parallel plexiglass slide using the Exakt 7210 VLC system. Longitudinal sections of the sample were then cut (200–300 μm) using a diamond precision parallel saw (Exakt-Apparatebau Hermann, Norderstedt, Germany). The cut slides were subjected to grinding (50–100μm) and polishing (Exakt 400 CS, AW 110) and viewed using a fluorescent microscope (Leica DMI6000B, Buffalo Grove, IL). Prepared slides were imaged for polyfluorochrome stains using filter cubes (ex/em: L5 480/527, N3 546/600, Chroma 425/475LP). Image channels were merged in red-green-blue profiles corresponding to the 2-, 4-, and 6-week bone front with an additional layer for phase contrast imaging of the final bone front at 8 weeks. All bone fronts

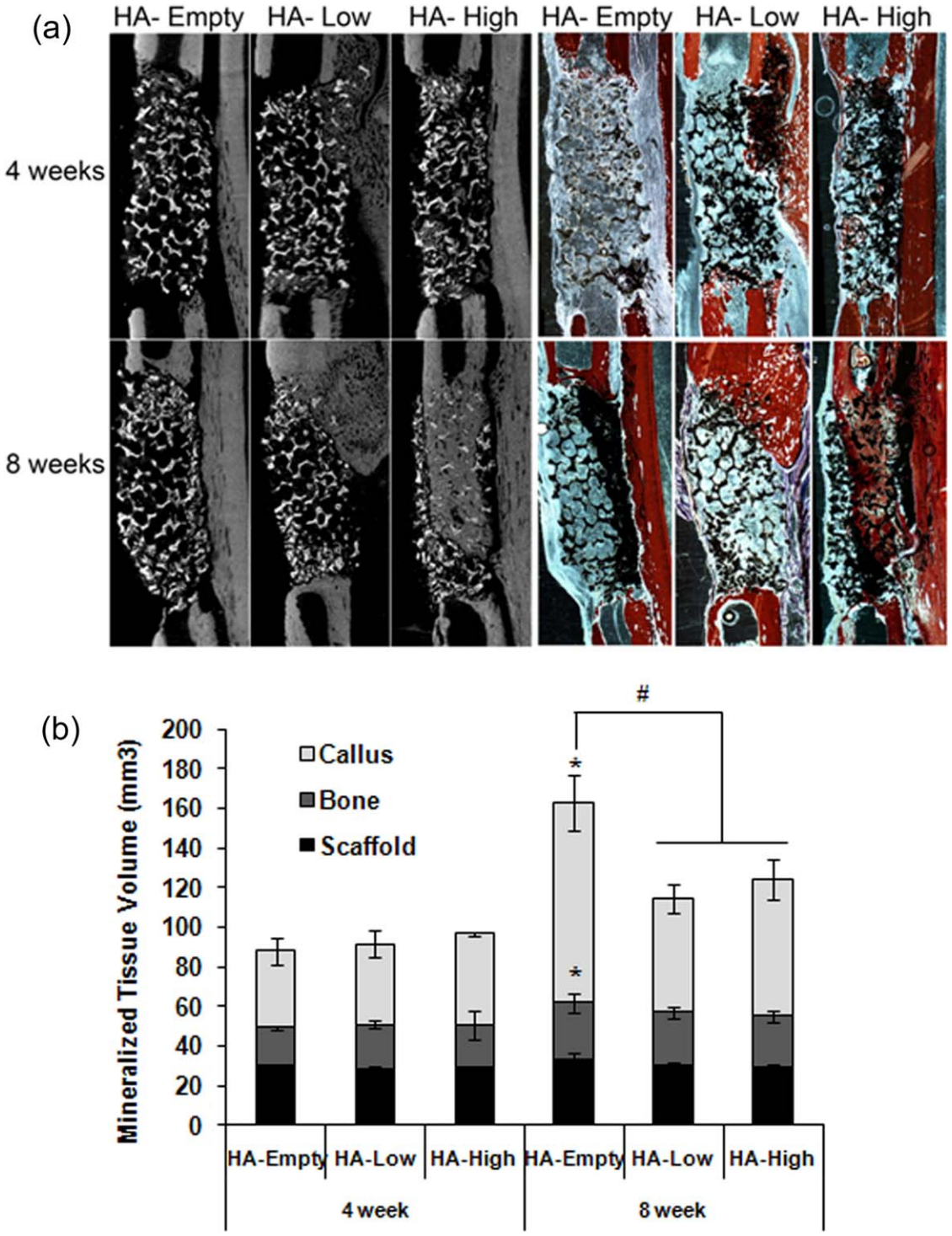

FIGURE 2. μCT of defects: (a) longitudinal μCT cross sections of the treated rabbit radius defect after 4 and 8 weeks show diffuse bone formation at 4 weeks and more mature ossified tissue within the scaffolds after 8 weeks. In addition to proximal and distal growth fronts, significant callus ossification is also observed. (b) Three-dimensional tissue volume measurement from μCT data indicated comparable bone volume within the scaffolds in all three treatment groups after 4 and 8 weeks. However, the callus bone volume was significantly greater in the control group than in the low cell density group after 8 weeks. Bone within the scaffold ($p = 0.016$) and in the callus ($p < 0.001$) increased significantly in the no cell group from 4 to 8 weeks (*). After 8 weeks, the callus mineralization of HA-empty was significantly greater (#) than that of the HA-low ($p = 0.003$) and HA-high ($p = 0.049$) groups. [Color figure can be viewed in the online issue, which is available at wileyonlinelibrary.com].

were identified corresponding to the infiltration depth into the scaffold. Bone front measurements were obtained by using histomorphometry (Bioquant Osteo, Nashville, TN). All measurements were distances from the defect origin (original saw cut) to the farthest continuous presence of fluorescence labeling. Total infiltration length included both

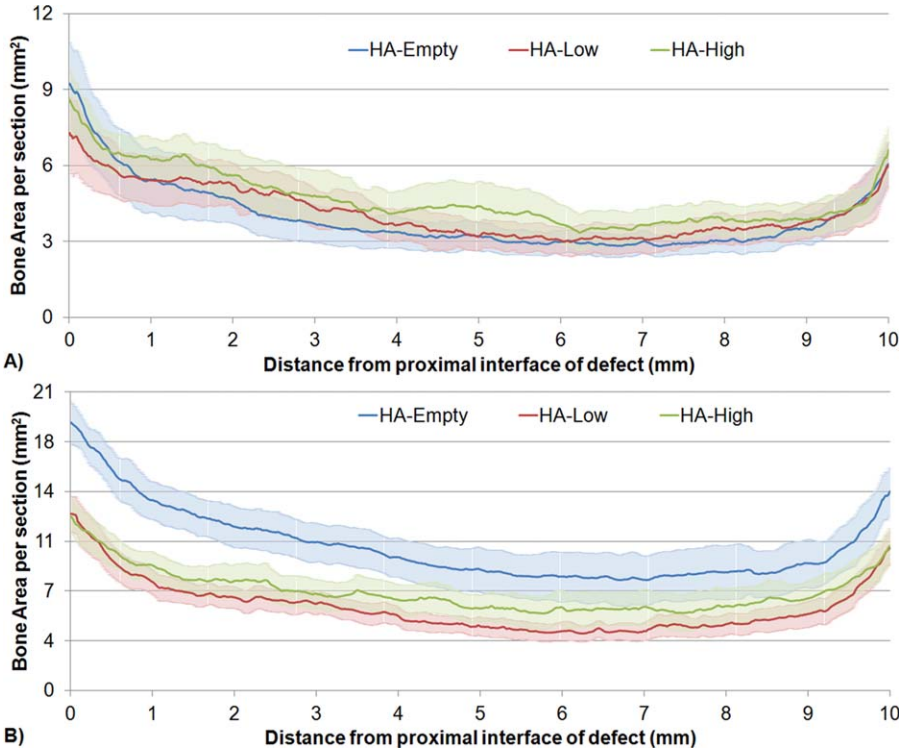

FIGURE 3. The distribution of ossified callus around the scaffold within the defect space after (a) 4 and (b) 8 weeks indicated that while the cell-seeded groups showed uniform callus ossification throughout the length of the defect, within the empty scaffold group there was greater ossification around the interfaces. [Color figure can be viewed in the online issue, which is available at wileyonlinelibrary.com].

proximal and distal growth fronts. Diffuse bone formation was classified as labeled bone occurring within the scaffold but not directly connected to the proximal or distal bone fronts and was excluded from the infiltration length measurements.

Micro-CT evaluation

Following killing, μCT analyses were performed on all samples before histological evaluation. Micro-CT analysis was performed using Skyscan 1076 (Skyscan) at an 8.77-μm pixel resolution while hydrated with formalin. The images were reconstructed with NRecon software (Skyscan) to generate gray-scale images ranging from 0 to 255, which was equivalent to the density range of 0.81 to 3.34 gm/cm^3. The μCT reconstructed axial slices were then evaluated by using CT software (Skyscan) to determine the bone regeneration patterns *in vivo* in terms of growth profiles and overall bone volume. New bone evaluation was based on differences in density between the scaffold (2.5 gm/cm^3 mean) and the newly forming osteoid or remodeling native bone (1.2–1.7 gm/cm^3). The μCT images were correlated with corresponding Alizarin Red-stained histological slides to confirm appropriateness of thresholds. The volume of interest was a 3D volume that extended over the 10-mm defect space created at the time of surgery. Unique regions of interest were defined for the ulna and the defect space occupied by the scaffold by manually circumscribing the external perimeter of the ulna and scaffold space every 0.2 mm over the 10-mm defect and interpolating between selections. New bone formation around the scaffold that was outside these regions was measured as the callus bone volume. The callus mineralized tissue area in each 8.77-μm section of this 10-mm defect space was computed for all three treatments to observe the trends in callus mineralization along the length of the defect from the proximal to the distal interface. Within the defect region of interest, the total bone regenerated within the scaffold and the total scaffold volume were independently measured.

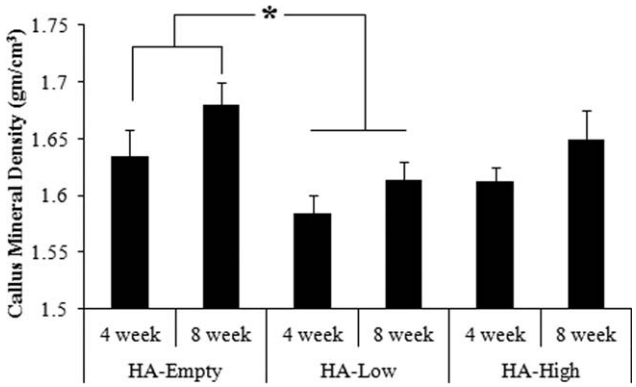

FIGURE 4. The mineralized tissue density of the callus volume after 4 and 8 weeks for the control, low, and high cell-seeded groups. There was a significant difference (*) between the HA-empty and HA-low ($p = 0.013$) and across all groups between 4 and 8 weeks ($p = 0.024$).

Statistical analysis

The normal distribution of the data was evaluated with the Shapiro-Wilk Normality Tests and verified with quantile

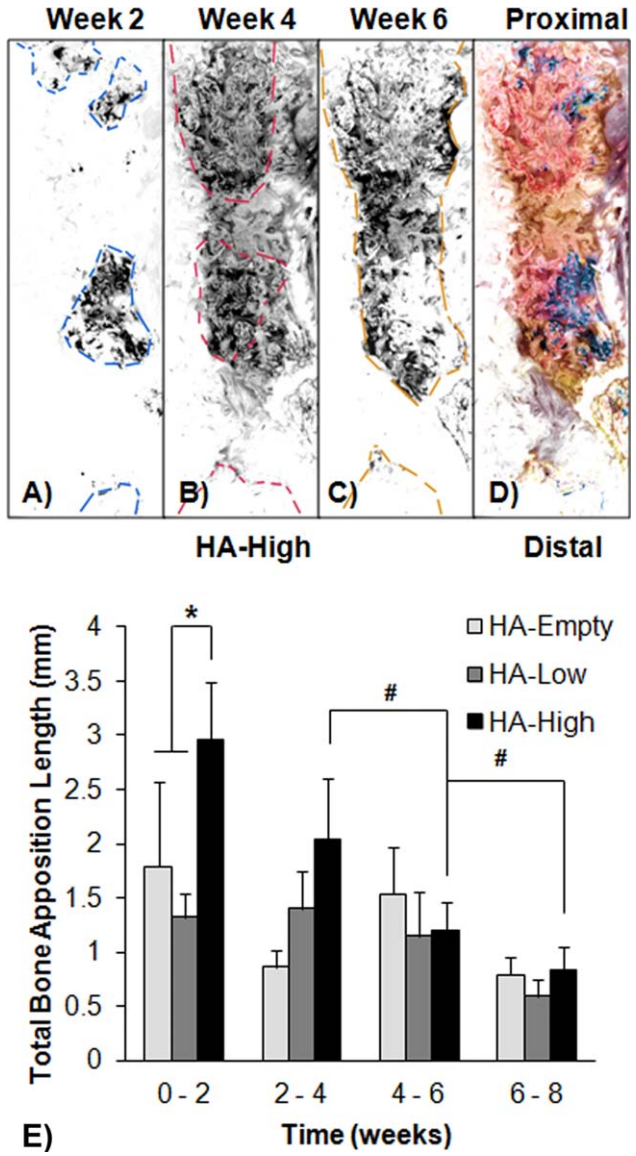

FIGURE 5. (a) Fluorochromes injected to assess bone formation after 2 (blue), 4 (red), and 6 (orange) weeks indicated continued bone infiltration and infiltration in HA-empty (a), HA-low (b), and HA-high (c) groups at both interfaces and over each 2-week period. (e) Total bone infiltration length as a function of time between labels. HA-high scaffolds demonstrated an increase (*) in infiltration from week 0 to 2 compared with HA-low and HA-empty groups ($p < 0.05$). The rate of bone infiltration decreased significantly in the HA-high group between the 2- to 4-, 4- to 6-, and 6- to 8-week time points (#). [Color figure can be viewed in the online issue, which is available at wileyonlinelibrary.com].

plots. Significance differences in μCT volume, area and mineral density measures, and quantitative histological analyses reported were determined using two-way analysis of variance (ANOVA), with a Tukey's test for *post hoc* evaluation. Significance in relative change from 4 to 8 weeks was determined using one-way ANOVA and Tukey's test for *post hoc* evaluation. Significance levels were set at $p < 0.05$ for all statistical measures reported. All data was reported as mean ± standard error of the mean.

RESULTS

Scaffold characterization

The scaffolds used in this study had a mean scaffold porosity of 65.5 ± 4.5% as indicated by the helium pycnometry and corroborated by the μCT analysis (65.48 ± 4.7%). The μCT morphometric analysis also indicated that the trabecular thickness of the scaffolds was 209 ± 7 μm, the trabecular spacing, which corresponds to pore size was 440 ± 40 μm, and the scaffold surface to volume ratio was 16.9 ± 1.3 mm^{-1}.

Cell characterization and scaffold seeding

The differentiation potential of the rabbit bone marrow-derived MSCs was confirmed using standard histological techniques for confirming osteogenic and adipogenic potentials [Fig. 1(a,b)]. The cells stained positive for Oil Red-O and Alizarin Red indicative of their multidifferentiation potential. The effectiveness of the scaffold seeding was demonstrated by using human bone marrow stromal cells. As shown in Figure 1(c), cell number was greater than control by 8 days after seeding and remained elevated *in vitro* through 22 days after seeding. The presence of viable, proliferation-competent cells 24 h after seeding verified the success of the cell seeding procedure.

Micro-CT evaluation

There were three distinct fronts of bone formation: from the proximal interface, the distal interface, and the interosseous syndesmosis that spanned from the ulna to the radius, similar to previous observations.[18] As shown in Figure 2(a,b), the regenerated bone volume within the scaffold as well as the callus volume increased for all groups between 4 and 8 weeks and were significantly different at 8 weeks in the HA-empty group ($p < 0.05$). There was no significant difference between groups in terms of bone formation within the scaffold at 4 or 8 weeks [Fig. 2(b)]. Figure 2(b) shows that the callus volume was significantly greater in HA-empty than in both the HA-high ($p = 0.02$) and HA-low ($p = 0.003$) groups at 8 weeks after implantation. Correspondingly, the rate of callus formation between 4 and 8 weeks was significantly higher in HA-empty than in HA-low or HA-high ($p < 0.05$) groups. The spatial callus regeneration patterns across the length of the scaffold indicated that all groups showed greater callus volume at the interfaces when compared with the interior. In addition, all groups showed greater callus formation at the proximal interface than at the distal interface, a trend that was most prominent in the HA-empty group. After 4 weeks, a paired analysis indicated that HA-high > HA-low > HA-empty group in terms of callus formation [Fig. 3(a)]. However, after 8 weeks' implantation, the callus formation in the HA-empty > HA-high > HA low group for every location across the length of the scaffold [Fig. 3(b)]. These trends indicated that the observed differences in callus formation rates between groups were not simply due to interfacial fronts of ossification. The measured callus density within all groups was significantly greater at 8 weeks than at 4 weeks. In addition, the callus density in HA-empty was significantly greater at

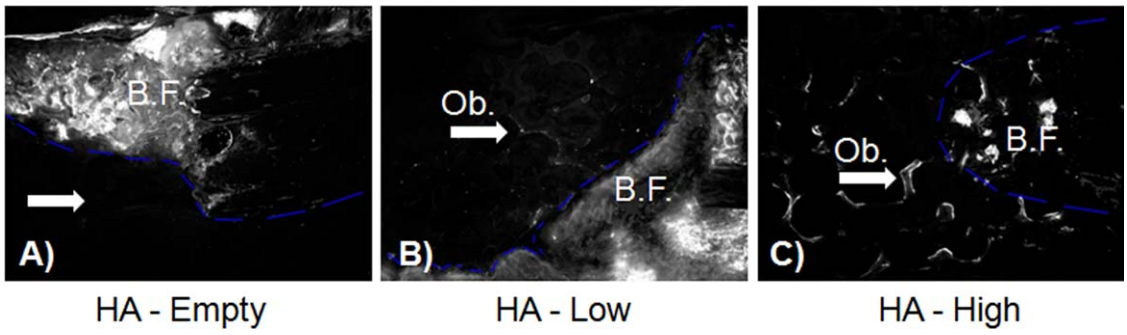

FIGURE 6. Fluorescence indicative of osteoid bone (white arrows, Ob.) was observed in proximity to scaffolds but not within bone front (demarcated by blue dash, B.F.). Empty scaffolds (a) demonstrated limited formation of diffuse labeled osteoid (within defect but not adjacent to the bone front) while both low (b) and high (c) cell-seeding demonstrated strong evidence of bone formation initiating directly from the scaffold surface. [Color figure can be viewed in the online issue, which is available at wileyonlinelibrary.com].

both 4 and 8 weeks than HA-low but not HA-high (Fig. 4) groups.

Fluorescence histomorphometry

Using longitudinal cross sections of the scaffolds, the length of bone infiltration was measured from the original defect cut to the farthest continuous presence of fluorescence labeling occurring at weeks 2, 4, and 6 [Fig. 5(a–e)], with final measurement of the bone front identified by phase contrast imaging at 8 weeks. The HA-high group had a significantly higher rate of bone infiltration than the HA-empty group at 2 weeks but not at any other time point [Fig. 5(b), $p < 0.05$]. In addition, the high-cell group showed a significant reduction from 4 to 6 and 6 to 8 weeks in infiltration length [Fig. 5(e)]. Diffuse bone, bone not directly connected to the bone fronts or included in infiltration length measurements, was observed where fluorescence labels were found surrounding scaffold struts [Fig. 6(a–c)] distributed through the interior of the scaffold. The osteoid shown in these figures corresponded with the single layer of bone cells found only at the 2-week time point and was found extensively in the cell-seeded HA groups as measured by the presence or absence of label distinct from the bone front in each sample (Table I).

DISCUSSION

The primary objective of this study was to determine whether the addition of BMSCs would accelerate bone regeneration in a rabbit radius segmental defect model.

TABLE I. Diffuse Bone Formation Unconnected With the Infiltrating Bone Front (Representative Images in Fig. 6) Is Present in Cell-Seeded Scaffold

Group	Samples With Diffuse Bone (N)	Percentage
HA-empty	1/6	12.5
HA-low	9/10	90.0
HA-high	8/8	100.0

Scaffolds were analyzed for the presence or absence of bone formation directly on the scaffold surface unconnected with the infiltrating bone fronts.

Based on a number of previous findings[3,6,23–26] indicating improved healing when BMSCs were used to augment bone repair using a variety of scaffolds and defect models, the hypothesis for this study was that BMSCs would also accelerate healing when used in combination with HA scaffolds in the rabbit radius segmental defect. In addition, the secondary objective was to determine the effect of seeding density on bone regeneration. The major findings from this study included (1) no significant benefit of seeding HA scaffolds with BMSCs in terms of regenerated bone volume within the scaffold, (2) a significant increase in callus volume in empty scaffolds as compared to cell-seeded scaffolds at 8 weeks after implantation, and (3) an increased rate of bone apposition in the initial 2 weeks after implanting the defect with HA-high scaffolds.

A number of studies supported a role for improved bone healing when BMSCs were used to augment HA scaffolds in sheep long-bone defects[3,23,24,27] and in a rabbit radial defect.[25,28] Noteworthy differences between previous studies and the current study included the lack of osteogenic induction, choice of evaluation time point, and use of a nonhealing defect. For example, a more challenging radial defect (1.5 cm) in rabbits and the inclusion of the osteogenic induction of cells was reported to improve bone regeneration at 3 months after implantation when compared with control nonseeded scaffolds.[25] Although the current findings are in contrast to a number of studies demonstrating improved bone regeneration with cell seeding, our results parallel that of Rai et al.[8] in that *in vitro* survivability and expansion were observed, but the transplantation of undifferentiated MSCs failed to improve bone volume *in vivo*. Similarly, uncultured BMSCs seeded on poly(L-lactic acid) scaffolds improved bone regeneration in a calvarial defect model; however, no added benefit was realized when cells were seeded on HA scaffolds.[29] Overall, the current findings are in agreement with the contention that the differentiation state and conditions under which cells are culture expanded before implantation influence regenerative potential.[10,12] The increase in the rate of bone infiltration with HA-high scaffolds is in agreement with the observation that HA scaffolds seeded with MSCs played a major role in the early stages of osteogenesis.[10,11,30] Under the conditions

of the current study, it is possible that the increased bone infiltration rate may be due to implanted MSCs having a positive effect on early cell recruitment, but thereafter interrupted the normal spatiotemporal cascade of bone healing through the rest of the study period. This speculation is supported by observations of a greater increase in callus volume and rate of callus formation in the HA-empty group at 4 and 8 weeks when compared with cell-seeded HA groups. Alternatively, it is also possible that the higher rate of bone formation in the HA-high group may be due to the seeded cells already being present in the scaffolds and bypassing the need for cell migration and the recruitment of endogenous osteogenic cells. This speculation is supported by the observed difference in callus distribution along the length of the implant between cell-seeded HA scaffolds and HA-empty scaffolds at 8 weeks after implantation. More specifically, greater callus content was observed proximally with HA-empty scaffolds when compared with cell-seeded HA scaffolds, alluding to the possibility that the migratory osteogenic cells contributed to this outcome. With the secondary objective to determine the effect of seeding density on bone regeneration, the cell densities selected for this study were similar to the minimal and optimal number of cells used by other investigators to measure bone formation in an ectopic model.[13] Based on the results of this study, the high cell density was sufficient to accelerate bone deposition through 2 weeks after implantation but was not sufficient to ultimately cause an increase in bone volume at 4 or 8 weeks. In contrast, the low seeding density was not sufficient to influence either of these parameters. In comparison with HA-empty scaffolds, limited callus formation was also observed when HA scaffolds were seeded with either high and low cell densities. These observations were in agreement with previous studies on the effect of cell seeding densities on mineralization *in vitro* using PCL-TCP scaffolds[14] and *in vivo* bone formation using calcium phosphate scaffolds.[31] Other observations included the diffuse or distributed bone formation on the interior surfaces of the scaffold and not stemming from the interfacial or interosseous bone fronts. It was observed that diffuse bone formation occurred in all but one of the cell-seeded scaffolds when compared with only one of the HA-empty scaffolds. When considered in conjunction with μCT analyses, this suggests that cell seeding led to the initiation of bone formation in discrete areas that did not significantly contribute to a substantial quantity of bone volume within the scaffold.

CONCLUSION

In this study, porous-interconnected HA scaffolds were seeded with BMSCs, and the construct was implanted in a rabbit radius segmental defect model to test the hypothesis that cell-seeded HA scaffolds improve bone regeneration. In addition, the effect of seeding density on bone regeneration was determined using two different cell-seeding densities. Although high cell seeding on HA scaffolds was observed to increase the rate of bone apposition in the initial 2 weeks after implantation, it was concluded from this study that the seeding of HA scaffolds with MSCs offered little to no benefit in increasing regenerated bone volume within the scaffold, increasing callus volume, or increasing rate of callus formation.

ACKNOWLEDGMENTS

The opinions and assertions contained herein are the private views of the authors and are not to be construed as official or reflecting the views of the Department of the Army or Department of Defense. This study was supported by the U.S. Army Medical Research and Material Command and of the Department of Defense.

REFERENCES

1. LeGeros RZ. Properties of osteoconductive biomaterials: calcium phosphates. Clin Orthop Relat Res 2002:81–98.
2. Giannoudis PV, Dinopoulos H, Tsiridis E. Bone substitutes: an update. Injury 2005;36:S20–S27.
3. Chistolini P, Ruspantini I, Bianco P, Corsi A, Cancedda R, Quarto R. Biomechanical evaluation of cell-loaded and cell-free hydroxyapatite implants for the reconstruction of segmental bone defects. J Mater Sci Mater Med 1999;10:739–742.
4. Goshima J, Goldberg VM, Caplan AI. The osteogenic potential of culture-expanded rat marrow mesenchymal cells assayed in vivo in calcium phosphate ceramic blocks. Clin Orthop Relat Res 1991: 298–311.
5. Matsushima A, Kotobuki N, Tadokoro M, Kawate K, Yajima H, Takakura Y, Ohgushi H. In vivo osteogenic capability of human mesenchymal cells cultured on hydroxyapatite and on beta-tricalcium phosphate. Artif Organs 2009;33:474–481.
6. Quarto R, Mastrogiacomo M, Cancedda R, Kutepov SM, Mukhachev V, Lavroukov A, Kon E, Marcacci M. Repair of large bone defects with the use of autologous bone marrow stromal cells. N Engl J Med 2001;344:385–386.
7. Lyons FG, Al-Munajjed AA, Kieran SM, Toner ME, Murphy CM, Duffy GP, O'Brien FJ. The healing of bony defects by cell-free collagen-based scaffolds compared to stem cell-seeded tissue engineered constructs. Biomaterials 2010;31:9232–9243.
8. Rai B, Lin JL, Lim ZX, Guldberg RE, Hutmacher DW, Cool SM. Differences between in vitro viability and differentiation and in vivo bone-forming efficacy of human mesenchymal stem cells cultured on PCL-TCP scaffolds. Biomaterials 2010;31:7960–7970.
9. Caplan AI. Why are MSCs therapeutic? New data: new insight. J Pathol 2009;217:318–324.
10. Tortelli F, Tasso R, Loiacono F, Cancedda R. The development of tissue-engineered bone of different origin through endochondral and intramembranous ossification following the implantation of mesenchymal stem cells and osteoblasts in a murine model. Biomaterials 2010;31:242–249.
11. Tasso R, Fais F, Reverberi D, Tortelli F, Cancedda R. The recruitment of two consecutive and different waves of host stem/progenitor cells during the development of tissue-engineered bone in a murine model. Biomaterials 2010;31:2121–2129.
12. Tasso R, Gaetani M, Molino E, Cattaneo A, Monticone M, Bachi A, Cancedda R. The role of bFGF on the ability of MSC to activate endogenous regenerative mechanisms in an ectopic bone formation model. Biomaterials 2012;33:2086–2096.
13. Kruyt M, de Bruijn J, Rouwkema J, Van Bliterswijk C, Oner C, Verbout A, Dhert W. Analysis of the dynamics of bone formation, effect of cell seeding density, and potential of allogeneic cells in cell-based bone tissue engineering in goats. Tissue Eng Part A 2008;14:1081–1088.
14. Zhou YF, Sae-Lim V, Chou AM, Hutmacher DW, Lim TM. Does seeding density affect in vitro mineral nodules formation in novel composite scaffolds? J Biomed Mater Res 2006;78:183–193.
15. Kim K, Dean D, Mikos AG, Fisher JP. Effect of initial cell seeding density on early osteogenic signal expression of rat bone marrow stromal cells cultured on cross-linked poly(propylene fumarate) disks. Biomacromolecules 2009;10:1810–1817.

16. Patterson TE, Kumagai K, Griffith L, Muschler GF. Cellular strategies for enhancement of fracture repair. J Bone Joint Surg Am 2008;90(suppl 1):111–119.
17. Appleford MR, Oh S, Oh N, Ong JL. In vivo study on hydroxyapatite scaffolds with trabecular architecture for bone repair. J Biomed Mater Res A 2009;89:1019–1027.
18. Guda T, Walker JA, Pollot BE, Appleford MR, Oh S, Ong JL, Wenke JC. In vivo performance of bilayer hydroxyapatite scaffolds for bone tissue regeneration in the rabbit radius. J Mater Sci Mater Med 2011;22:647–656.
19. Guda T, Walker JA, Singleton BM, Hernandez JW, Son JS, Kim SG, Oh DS, Appleford MR, Ong JL, Wenke JC. Guided bone regeneration in long-bone defects with a structural hydroxyapatite graft and collagen membrane. Tissue Eng Part A. 2012 Sep 14.
20. Muschler GF, Boehm C, Easley K. Aspiration to obtain osteoblast progenitor cells from human bone marrow: the influence of aspiration volume. J Bone Joint Surg Am 1997;79:1699–1709.
21. Parr JA, Young T, Dunn-Jena P, Garetto LP. Histomorphometrical analysis of the bone-implant interface: comparison of microradiography and brightfield microscopy. Biomaterials 1996;17:1921–1926.
22. Sudmann E, Bang G. Indomethacin-induced inhibition of haversian remodelling in rabbits. Acta Orthop Scand 1979;50(6 Pt 1): 621–627.
23. Petite H, Viateau V, Bensaid W, Meunier A, de Pollak C, Bourguignon M, Oudina K, Sedel L, Guillemin G. Tissue-engineered bone regeneration. Nat Biotechnol 2000;18:959–963.
24. Viateau V, Guillemin G, Bousson V, Oudina K, Hannouche D, Sedel L, Logeart-Avramoglou D, Petite H. Long-bone critical-size defects treated with tissue-engineered grafts: a study on sheep. J Orthop Res 2007;25:741–749.
25. Niemeyer P, Szalay K, Luginbuhl R, Sudkamp NP, Kasten P. Transplantation of human mesenchymal stem cells in a non-autogenous setting for bone regeneration in a rabbit critical-size defect model. Acta Biomater 2010;6:900–908.
26. Zhu L, Liu W, Cui L, Cao Y. Tissue-engineered bone repair of goat-femur defects with osteogenically induced bone marrow stromal cells. Tissue Eng 2006;12:423–433.
27. Kon E, Muraglia A, Corsi A, Bianco P, Marcacci M, Martin I, Boyde A, Ruspantini I, Chistolini P, Rocca M, Giardino R, Cancedda R, Quarto R. Autologous bone marrow stromal cells loaded onto porous hydroxyapatite ceramic accelerate bone repair in critical-size defects of sheep long bones. J Biomed Mater Res 2000;49:328–337.
28. Kasten P, Luginbuhl R, van Griensven M, Barkhausen T, Krettek C, Bohner M, Bosch U. Comparison of human bone marrow stromal cells seeded on calcium-deficient hydroxyapatite, beta-tricalcium phosphate and demineralized bone matrix. Biomaterials 2003;24:2593–2603.
29. Kretlow JD, Spicer PP, Jansen JA, Vacanti CA, Kasper FK, Mikos AG. Uncultured marrow mononuclear cells delivered within fibrin glue hydrogels to porous scaffolds enhance bone regeneration within critical-sized rat cranial defects. Tissue Eng Part A 2010;16:3555–3568.
30. Tasso R, Augello A, Boccardo S, Salvi S, Caridà M, Postiglione F, Fais F, Truini M, Cancedda R, Pennesi G. Recruitment of a host's osteoprogenitor cells using exogenous mesenchymal stem cells seeded on porous ceramic. Tissue Eng Part A 2009;15:2203–2212.
31. van Gaalen SM, de Bruijn JD, Wilson CE, Wilson CE, van Blitterswijk CA, Verbout AJ, Alblas J, Dhert WJ. Relating cell proliferation to in vivo bone formation in porous Ca/P scaffolds. J Biomed Mater Res 2010;92:303–310.